

The *Treponema pallidum* tro Operon Encodes a Multiple Metal Transporter, a Zinc-dependent Transcriptional Repressor, and a Semi-autonomously Expressed Phosphoglycerate Mutase*[§]

Received for publication, January 23, 2003, and in revised form, March 31, 2003
Published, JBC Papers in Press, March 31, 2003, DOI 10.1074/jbc.M300781200

Karsten R. O. Hazlett^{‡§}, Frank Rusnak[†], David G. Kehres^{||}, Scott W. Bearden^{**‡‡},
Carson J. La Vake[‡], Morgan E. La Vake[‡], Michael E. Maguire^{||}, Robert D. Perry^{**},
and Justin D. Radolf^{‡§§}

From the [‡]Center for Microbial Pathogenesis and ^{§§}Departments of Medicine and Genetics & Developmental Biology, University of Connecticut Health Center, Farmington, Connecticut 06030-3710, the [¶]Department of Biochemistry and Molecular Biology, Mayo Clinic and Foundation, Rochester, Minnesota 55905, the ^{||}Department of Pharmacology, School of Medicine, Case Western Reserve University, Cleveland, Ohio 44106, and the ^{**}Department of Microbiology, Immunology, and Molecular Genetics, University of Kentucky, Lexington, Kentucky 40536

The *Treponema pallidum* tro operon encodes an ABC transporter (TroABCD), a transcriptional repressor (TroR), and the essential glycolytic enzyme phosphoglycerate mutase (Gpm). The apparently discordant observations that the solute binding protein (TroA) binds Zn²⁺, whereas DNA binding by TroR *in vitro* is Mn²⁺-dependent, have generated uncertainty regarding the identities of the ligand(s) and co-repressor(s) of the permease. Moreover, this operonic structure suggests that Gpm expression, and hence glycolysis, the sole source of ATP for the bacterium, would be suspended during TroR-mediated repression. To resolve these discrepancies, we devised an experimental strategy permitting a more direct assessment of Tro operon function and regulation. We report that (i) apo-TroA has identical affinities for Zn²⁺ and Mn²⁺; (ii) the Tro transporter expressed in *Escherichia coli* imports Zn²⁺, Mn²⁺, and possibly iron; (iii) TroR represses transporter expression in *E. coli* at significantly lower concentrations of Zn²⁺ than of Mn²⁺; and (iv) TroR-mediated repression causes a disproportionately greater down-regulation of the transporter genes than of *gpm*. The much higher concentrations of Zn²⁺ than of Mn²⁺ in human body fluids suggests that Zn²⁺ is both the primary substrate and co-repressor of the permease *in vivo*. Our data also indicate that Gpm expression and, therefore, glycolysis would not be abrogated when *T. pallidum* encounters high Zn²⁺ levels.

Treponema pallidum, the causative agent of syphilis, is a noncultivable sexually transmitted human pathogen that disseminates from a site of inoculation, usually within the genital area, to diverse organs where it can establish persistent, even lifelong, infection (1). Like all pathogens, *T. pallidum* presumably requires sequestered transition metals for vital structural and catalytic functions in proteins. Nevertheless, in contrast to other pathogenic bacteria in which specialized uptake systems for iron (2–4), and more recently for Zn²⁺ and Mn²⁺ (5–8), have been identified, there is little information about metal acquisition by the syphilis spirochete. The lack of techniques for *in vitro* cultivation and genetic manipulation of *T. pallidum* has greatly hindered investigation of treponemal physiology, including metal metabolism.

Two recent developments have spawned interest in the processes by which *T. pallidum* acquires trace metals. One is the availability of the genomic sequence of the spirochete (9), which reveals that many genes encoding well characterized iron-containing proteins (e.g. cytochromes, superoxide dismutase, and tricarboxylic acid metalloenzymes) are lacking. The finding that *T. pallidum* expresses at least two experimentally confirmed iron-binding proteins, superoxide reductase (neelaredoxin) and rubredoxin, (10–12), argues that the bacterium does require iron. The second impetus to study metal utilization by *T. pallidum* is provided by the discovery of the six gene tro (transport-related operon) (Fig. 1) (13). The first gene of the operon, troA, encodes the solute binding protein (SBP)¹ component of an ATP-binding cassette transporter (13–15) belonging to a newly described cluster (cluster nine or C9) of transition metal permeases (5). In addition to encoding an ATPase (TroB), two cytoplasmic membrane permeases (TroC and TroD), and a DtxR-like metalloregulator (TroR), the operon also encodes the glycolytic enzyme phosphoglyceromutase (Gpm) (13). Because the *T. pallidum* Gpm has no requirement for metals (16), the physiological benefit of transcriptionally linking the spirochete's sole copy of this essential enzyme to the Tro transporter genes is unclear.

The identity of the metal ligand(s) for the Tro transporter is a subject of controversy (5, 6). Our analysis of TroA purified from *Escherichia coli* showed that Zn²⁺ was present in a 1:1 molar ratio, whereas other metals were present in trace or

* This work was supported in part by National Institutes of Health Grants AI-10573 (to K. R. O. H.), AI-26756 (to J. D. R.), AI25098 (to R. D. P.), and GM61748 (to M. E. M.) and by funds from the Mayo Foundation (to F. R.). The costs of publication of this article were defrayed in part by the payment of page charges. This article must therefore be hereby marked "advertisement" in accordance with 18 U.S.C. Section 1734 solely to indicate this fact.

This paper is dedicated to our friend and colleague, Frank Rusnak, who passed on September 7, 2002. Frank selflessly offered his time, guidance, encouragement, and wisdom to all he met. We will greatly miss you, Frank.

[§] The on-line version of this article (available at <http://www.jbc.org>) contains a supplemental table and supplemental figures.

[†] Deceased.

[§] To whom correspondence should be addressed: Center for Microbial Pathogenesis, University of Connecticut Health Center, 263 Farmington Ave., Farmington, CT 06030-3710. Tel.: 860-679-8391; Fax: 860-679-8130; E-mail: KHazlett@up.uconn.edu.

^{‡‡} Present address: Div. of Vector-Borne Infectious Diseases, Centers for Disease Control and Prevention, Fort Collins, CO 80521.

¹ The abbreviations used are: SBP, solute binding protein; HRMM, Hazlett-Radolf minimal medium; PIPES, piperazine-*N,N'*-bis(2-ethanesulfonic acid); RT, reverse transcription; TPEN, *N,N,N',N'*-tetrakis(2-pyridyl-methyl)ethylenediamine.

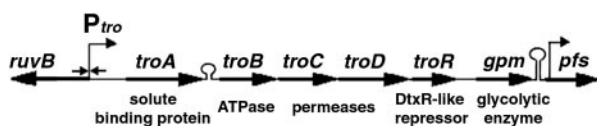


FIG. 1. Schematic diagram of the *tro* operon (13). Genes, promoters, and stem-loop structures are noted at the *top*; functions of the encoded proteins are listed at the *bottom*. Bent arrows indicate previously annotated promoters; inverted arrows indicate the TroR-binding site within the *tro* promoter (*P*_{tro}) (20). The stem-loop structure immediately downstream of *troA* is an attenuator, whereas the stem-loop downstream of *gpm* is a transcriptional terminator (13).

undetectable quantities (17). On the assumption that the SBP determines specificity of the transporter (18, 19), we proposed that the permease mediates Zn^{2+} influx (15). On the other hand, Posey *et al.* (20), using recombinant TroR for mobility shift DNA binding and DNase I footprint assays, reported that only Mn^{2+} could promote the binding of TroR to the *tro* promoter, leading them and others to conclude that the permease transports Mn^{2+} (5–7, 21–24). Conclusions from both studies are, however, essentially extrapolations from *in vitro* data. There are precedents for metalloproteins binding Zn^{2+} rather than their primary substrate when heterologously expressed in *E. coli* (25, 26). Similarly, *in vitro* and *in vivo* studies of metalloregulators have not always yielded identical profiles of metal-dependent DNA binding (3, 27, 28). We therefore devised an experimental strategy that would permit a more direct assessment of Tro permease function and regulation. Here we examined (i) metal binding by apo-TroA; (ii) the functional capacity of the transporter when expressed in surrogate hosts; (iii) the metal specificity of TroR-mediated transporter repression in *E. coli*; and (iv) the effect of TroR-mediated repression on Gpm expression. Our findings indicate that the permease transports Zn^{2+} , Mn^{2+} , and possibly iron but that Zn^{2+} is likely to be the primary activator of TroR under physiological conditions. We also found that expression of Gpm was not tightly linked to transcription of the *tro* transporter genes. This revised understanding of metal uptake and regulation by the Tro permease provides a foundation for further analysis of its role in treponemal metal metabolism and, by extension, syphilis pathogenesis.

EXPERIMENTAL PROCEDURES

Primers and Plasmids—Descriptions of the primers and plasmids used in this work are presented in the supplemental table, which is available online at the JBC web site (www.jbc.org).

Bacterial Strains and Media—Animal protocols described in this work were approved by the University of Connecticut Health Center Animal Care Committee under the auspices of Animal Welfare Assurance A3471-01. *T. pallidum* subspecies *pallidum* (Nichols-Farmington strain) was propagated by intratesticular inoculation of adult New Zealand White rabbits and harvested as described previously (29). Unless otherwise indicated, *E. coli* strain TOP10F' (Invitrogen) was the recipient strain for recombinant constructs and was grown in LB medium with appropriate antibiotic supplementation. For experiments requiring media with reduced metal contents, either M9 medium (Becton Dickinson, Sparks, MD) or a specially formulated minimal medium (Hazlett-Radolf minimal medium (HRMM)) was utilized for the growth of *E. coli*. M9 medium contains 1× M9 salts, 0.2% casamino acids, and 0.4% glucose. HRMM contains 0.4% glucose, 0.2% casamino acids, 0.2% ATP, 0.2% ammonium sulfate, 1 mM magnesium sulfate, 9 μ M $FeSO_4$, and 1.67% PIPES, pH 6.5. *Yersinia pestis* strains were grown in the defined medium PMH2 (30).

Generation of TroA apo Proteins and Determination of Dissociation Constants—The plasmid (pHTa:TroA), which encodes an isopropyl- β -D-thiogalactopyranoside-inducible polyhistidine-tagged TroA protein has been described previously (17). This plasmid also served as the template for site-directed mutagenesis (QuikChange, Stratagene, La Jolla, CA) with primers TroA H199E 5' and TroA H199E 3', which changed the H codon (CAT) of residue 199 to a E codon (GAA), generating pHTa:TroA(H199E). Sequence analysis confirmed that only the desired mutation had been introduced. Expression and purification of His-TroA

and His-TroA(H199E) were performed as previously described (17). His tags were removed by digestion with TEV protease (Invitrogen) followed by a second round of nickel-nitrilotriacetic acid chromatography, which captures free His tag, uncleaved fusion protein, and the His-tagged TEV protease. To generate apo-proteins suitable for metal binding studies, endogenously bound metals were removed from the purified proteins by overnight dialysis against 0.1 M sodium acetate buffer (pH 4.6) containing 10 mM 1,10 *o*-phenanthroline (Sigma) (31). Restoration of metal binding capacity was achieved by sequential dialysis against 0.1 M sodium acetate (pH 4.6) and 0.1 M sodium acetate (pH 6.5), respectively. The apo-proteins were adjusted to between 25 and 35 μ M and aliquoted as 1.1-ml portions into 8000 molecular weight cut-off dialysis bags (SPECTRA/POR, Spectrum Medical Industries, Inc, Los Angeles, CA). Thereafter, all protein manipulations employed acid-washed plastic containers and buffers treated with Chelex-100 (Bio-Rad). The dialysis bags containing apo-protein were transferred to 50-ml conical tubes containing 45 ml of 0.1 M sodium acetate (pH 6.5) with Mn^{2+} or Zn^{2+} acetate (0–100 μ M) and dialyzed overnight. Protein and dialysate samples were analyzed for Zn^{2+} by inductively coupled plasma emission spectroscopy or for Mn^{2+} by graphite furnace atomic absorption spectroscopy at the Mayo Clinic (Rochester, MN). The protein concentrations were confirmed by amino acid analysis. Metal-to-proteins ratios (θ) were plotted against the free metal (Me^{2+}) concentrations (μ M) and fitted to sigmoidal curves using the equation $\theta = ((N[Me^{2+}])/(K_d + [Me^{2+}])) + 0.3$, where N (Me^{2+} -binding sites) = 1 (17). The correction factor of 0.3 was included to better fit the sigmoidal curves to the data; K_d values obtained without this correction did not differ significantly from those presented in this work.

Y. pestis znu and mntH Mutants and Complementation Plasmids—To generate the *Y. pestis znu* knockout plasmid pSucZnu3.5, we recovered the wild type *znu* locus from a *Sau3AI* genomic library (32) using a *znuA* probe and subcloned a 9.4-kb *BglIII/Asp718* fragment into pWSK129, generating pZnu2, which served both as a complementation plasmid as well as an intermediate in the construction of pSucZnu3.5. pZnu2 was digested with *EcoRI* and *ApaI*, treated with Klenow, and self-ligated, generating pZnu3, which harbors the *znu* locus with a 1265-bp deletion covering approximately half of *znuB*, all of *znuC*, and the bi-directional *znuCB/znuA* promoter. The 7.5-kb Δ *znu XbaI* fragment from pZnu3 was ligated into the suicide vector pSuc1 (33), generating pSucZnu3.5, which was electroporated into *Y. pestis* KIM6+ (34). Clones arising from double cross-over events were selected by successively screening for ampicillin and sucrose resistance. A Δ *znu* isolate (KIM6–2077+) whose genotype was confirmed by Southern blot was used in this work. To generate a *mntH* knockout plasmid, the 5' and 3' regions of the *mntH* gene were PCR-amplified from *Y. pestis* DNA using primer pairs YpMntH5'-*SalI*/YpMntH5'-*SmaI*R and YpMntH3'-*SmaI*F/YpMntH3'-*SpeI*, digested with *SalI/SmaI* and *SmaI/SpeI*, respectively, and cloned in tandem into *SalI/SpeI*-digested suicide vector pKNG101 (35), creating pAMntH. The resulting insert consists of the *mntH* gene, lacking 600 bp of coding sequence, flanked by 300 and 80 bp at the 5' and 3' ends, respectively. Plasmid pAMntH was used to transform *Y. pestis* KIM6 and the isogenic *yfe* mutant *Y. pestis* KIM6–2031.1 (34). Clones arising from double cross-over events were selected by successively screening for streptomycin and sucrose resistance. Plasmid pMntH-Op was generated by PCR amplifying the *mntH* gene with its native promoter from *Y. pestis* KIM6 DNA using primer pair YpMntH5'-*SalI*/YpMntH3'-*XbaI*; the resulting fragment was cloned into pWSK129 (36) in the opposite orientation of the vector-encoded *lacZ* gene.

Construction of Permease Plasmids—The promoter-less *troABCD* genes were PCR-amplified from *T. pallidum* chromosomal DNA using the proofreading polymerase Ex-Taq (Panvera, Madison, WI), primers NoPro TroA 5' *EcoRI* and TroD 3' *EcoRI* and cloned into TOPO pCR2.1 (Invitrogen). Following sequence confirmation, the insert was moved into the *EcoRI* site of pBAD18 (37), and a plasmid harboring the treponemal genes in the same orientation as the pBAD promoter (pTroA-D) was identified. pTroA(H199E)-D was generated from pTroA-D as described above and confirmed by sequence analysis. The primer pairs used for PCR amplify *mntH*, *yfeABCD*, *scaCBA*, and *adcCBA* from *E. coli* K-12, *Y. pestis* KIM6, *S. gordonii* DL1, and *Streptococcus pneumoniae* TIGR 4 genomic DNAs, respectively, for cloning into pBAD18, are presented in the supplemental table, as are the resulting plasmids. The divergently transcribed *znu* genes of *E. coli* K12 were amplified using primers Ec ZnuA 3' *KpnI* and Ec ZnuB 3' *XbaI*, digested, and directly cloned into *KpnI/XbaI*-digested pWSK129, generating pEcZnu.

To clone the complete *tro* operon, a DNA fragment extending from 106 bp upstream of the *troA* start codon to the *gpm* stop codon was

PCR-amplified from *T. pallidum* DNA using Ex-Taq polymerase (Panvera) and primers TroPro 5' *EcoRI* and Gpm 3' *SacII*. The amplicon was digested with *EcoRI* and *SacII* and cloned into the *EcoRI/SacII* sites of plasmids pWSK129 and pWSK29 (36) such that the *tro* operon was oriented oppositely to that of the vector-encoded *lacZ* promoter, creating pPro-Gpm and pPro-Gpm Amp, respectively. Transformants were plated on M9 agar containing 50 $\mu\text{g/ml}$ kanamycin (pPro-Gpm) or 100 $\mu\text{g/ml}$ ampicillin (pPro-GpmAmp), 0.1 mM isopropyl- β -D-thiogalactopyranoside, 20 $\mu\text{g/ml}$ 5-bromo-4-chloro-3-indolyl- β -D-galactopyranoside (X-gal) and grown overnight at 30 °C. The cloned insert was sequenced using primers listed in the supplemental materials. A variant, pNoPro-Gpm, which lacks the *tro* promoter, was similarly generated using primers NoPro TroA 5' *EcoRI* and Gpm 3' *SacII*.

Complementation of *Y. pestis* and *E. coli* Transporter Mutants—Complementation analysis of *Y. pestis* strains was conducted in PMH2 broth (30) and chelator gradient plates as described previously (34); all manipulations were conducted in acid-washed glassware. For experiments with broth, *Y. pestis* strains cultivated on tryptose blood agar slants were suspended in PMH2 medium to an A_{620} of 0.1 and grown overnight. The following morning they were diluted to an A_{620} of 0.1 in fresh PMH2 containing the required antibiotics with or without 0.2% arabinose. Growth at 30 °C in a shaking water bath was spectrophotometrically monitored. Arabinose-containing chelator gradient plates containing 0–1 μM TPEN or 0–5 μM conalbumin were inoculated and incubated for 3 days at 30 °C, after which growth into the metal-depleted zones was measured. Complementation analysis of a Zn^{2+} uptake-deficient *E. coli* strain was conducted in HRMM broth. Overnight HRMM cultures of *E. coli* GR354 ($\Delta\text{znu}/\Delta\text{zupT}$) (38) bearing either control or transporter plasmids were diluted into fresh medium containing appropriate antibiotics, 0 or 0.2% arabinose, and various concentrations of either the Zn^{2+} chelator TPEN or ZnCl_2 . The cultures were incubated at 37 °C with vigorous aeration, and growth was spectrophotometrically monitored for 12 h.

^{65}Zn and ^{54}Mn Transport Assays—With minor variation, transport assays were conducted as previously described (39, 40). *E. coli* strain MM2115 (ΔmntH) (40) and *E. coli* strain GR362, which lacks all known Zn^{2+} uptake and efflux transporters (38), were transformed with pBAD18 or pTroA-D. Overnight cultures were diluted into 0.4% fresh Chelex 100-treated tryptone, 0.25% NaCl broth, grown for 3 h, induced with 10 mM arabinose for 15–30 min, and added to isotope-containing broth (100 nM $^{65}\text{Zn}^{2+}$ (Perkin-Elmer, Boston, MA) or 50 nM $^{54}\text{Mn}^{2+}$ (Perkin-Elmer)). Culture samples, taken at intervals from 30 s to 5 min, were collected on 0.45- μm filters, rinsed twice with 5 ml of ice-cold medium, and processed for scintillation counting as described previously (39). Channels 401–945 were used to detect photons derived from γ radiation of ^{54}Mn , whereas all channels were used to detect photons derived from ^{65}Zn radiation.

Metal Sensitivity Assays—Overnight cultures were diluted 1:100 into fresh HRMM and plated on HRMM, 1% agarose plates containing 0.1 mg/ml ampicillin and either 0 or 0.2% L-arabinose. Sterile 6-mm paper disks (Becton Dickinson) were placed in the center of the air-dried plates and impregnated with 10 μl of 0.5 M ZnCl_2 , 1 M MnCl_2 , or 1 M FeSO_4 . Following overnight incubation at 37 °C, the zones of inhibition were measured in blinded fashion. The measurements from three to seven independent experiments were used to calculate the mean zones of inhibition. The differences in mean zone sizes were compared using the two-tailed Student's *t* test; *p* values ≤ 0.01 were considered significant. Although Fe^{2+} (FeSO_4) was used in these assays, the lability of this ion under aerobic conditions likely allowed for oxidation to the Fe^{3+} ion.

Immunologic Reagents and Immunoblot Analysis—Polyclonal rat antiserum directed against TroA has been previously described (14). Antiserum was adsorbed with *E. coli* (pWSK129) lysates that had been electrophoresed on a 12.5% SDS-polyacrylamide gel and electrotransferred to nitrocellulose. A mouse monoclonal antibody directed against *E. coli* σ^{70} was purchased from NeoClone Biotechnology (Madison, WI). To produce antisera directed against Gpm and TroR, the *T. pallidum* *gpm* and *troR* genes were amplified using primer pairs Gpm 5' *NcoI*/Gpm 3' *EcoRI* and TroR 5' *NcoI*/TroR *EcoRI*, digested with *NcoI* and *EcoRI*, and cloned into the expression vector pProExHTa (Invitrogen). The resulting plasmids (pHTa:Gpm and pHTa:TroR) encode isopropyl- β -D-thiogalactopyranoside-inducible polyhistidine-tagged proteins, which were purified from induced *E. coli* cell lysates by nickel-nitrilotriacetic acid chromatography and used to immunize 4-week-old male Sprague-Dawley rats as previously described (29). *T. pallidum*, *E. coli*, and *Y. pestis* lysates were resolved on 12.5% SDS-polyacrylamide gels and electrotransferred to nitrocellulose. The blots were incubated with 1:1000 to 1:5000 dilutions of the appropriate antiserum or anti- σ^{70}

monoclonal antibody and then probed with a 1:30,000 dilution of horseradish peroxidase-conjugated goat anti-rat (or anti-mouse) (Southern Biotechnology Associates, Birmingham, AL). The immunoblots were developed using the SuperSignal Femto chemiluminescence substrate (Pierce) followed by exposure to film (Amersham Biosciences). In the metal repression studies, the densitometric signals of immunoreactive bands were measured by an Alpha Innotech ChemImager 4400 (Alpha Innotech Corporation, San Leandro, CA).

Detection of *tro* Transcripts by RT-PCR—RNAs were isolated using Trizol (Invitrogen) and treated with RQ1 RNase-free DNase (Promega, Madison, WI) until the RNAs were free of contaminating DNA. RT-PCR reactions were performed with the Titan One-Step RT-PCR kit (Roche Applied Science) as previously described (10) using the RT-PCR primers listed in the supplemental table. For each primer set, three reactions were performed: (i) RT-PCR with RNA template, (ii) PCR with RNA template, and (iii) PCR with control template DNA. In reactions without RT, the Expand High Fidelity DNA polymerase (Roche Applied Science) was substituted for the RT/DNA polymerase enzyme mixture. Following the RT reaction (50 °C for 30 min), PCR was performed using the following parameters: 98 °C for 2 min followed by 30 cycles of 94 °C for 5 s; 63 °C for 10 s; and 68 °C for 45 s followed by a single terminal extension at 68 °C for 3 min. Densitometry was performed as above.

RESULTS

Apo-TroA binds Zn^{2+} and Mn^{2+} with Equal Affinity—TroA purified from *E. coli* contains 0.96 Zn^{2+} atoms/protein molecule (17). However, this result could reflect the relatively high level of Zn^{2+} in *E. coli* (41) rather than the intrinsic metal binding capability of the protein. We therefore measured the affinity of purified de-metalled recombinant TroA (apo-TroA) for Zn^{2+} and Mn^{2+} . This apo-protein retains native structure as determined by x-ray crystallography (31). Inductively coupled plasma emission spectroscopy showed that apo-TroA contained an average of 0.07 ± 0.02 Zn^{2+} atoms/TroA. In preliminary studies using 100-fold molar excesses of Zn^{2+} or Mn^{2+} , apo-TroA bound similar amounts of either cation, 0.901 atoms of Zn^{2+} /TroA or 0.866 atoms of Mn^{2+} /TroA. Binding studies were then performed in which apo-TroA was dialyzed against concentrations of Zn^{2+} or Mn^{2+} between 0 and 100 μM . The measured metal-to-protein ratios (two independent experiments/metal) were plotted against the free metal concentrations (Fig. 2A). The calculated K_d values for Zn^{2+} and Mn^{2+} (1.27 ± 0.4 and 0.95 ± 0.2 μM , respectively) indicate that TroA has virtually identical affinities for the two metals.

X-ray crystal structures have been solved for two C9 SBPs, TroA of *T. pallidum* and PsaA of *Streptococcus pneumoniae* (15, 42). In TroA, Zn^{2+} is coordinated by residues His⁶⁸, His¹³³, His¹⁹⁹, and Asp²⁷⁹; the corresponding residues in PsaA are His⁶⁷, His¹³⁹, Glu²⁰⁵, and Asp²⁸⁰. Alignment of amino acid sequences of C9 SBPs with experimentally confirmed metal ligands (see supplemental Fig. S1) showed that His^{68/67} and His^{133/139} are strictly conserved, residue 279/280 is either Asp or Glu, whereas residue 199/205 is either His or Glu. C9 SBPs with His at the 199/205 position tend to bind Zn^{2+} , whereas those with Glu at this position predominantly bind Mn^{2+} or iron, suggesting that the identity of residue 199/205 could be a critical determinant of ligand specificity (15). We therefore mutated His¹⁹⁹ to Glu in TroA and measured the affinities of the mutant apo-protein for Zn^{2+} and Mn^{2+} . The mutation reduced the affinity of apo-TroA for Zn^{2+} by no more than 50% ($K_d = 2.64 \pm 0.8$ μM) but, surprisingly, abrogated its capacity to bind Mn^{2+} (Fig. 2B).

Functional Analysis of the Heterologously Expressed *Tro* Transporter—We next asked whether the *Tro* permease could mediate uptake of Zn^{2+} and/or Mn^{2+} . Because *T. pallidum* cannot be genetically manipulated, functional studies must be performed in a surrogate host. We therefore cloned the promoter-less *troABCD* genes downstream of the arabinose-inducible promoter of pBAD18 (37), creating pTroA-D (supplemental table). Immunoblot and RT-PCR analyses demonstrated that the

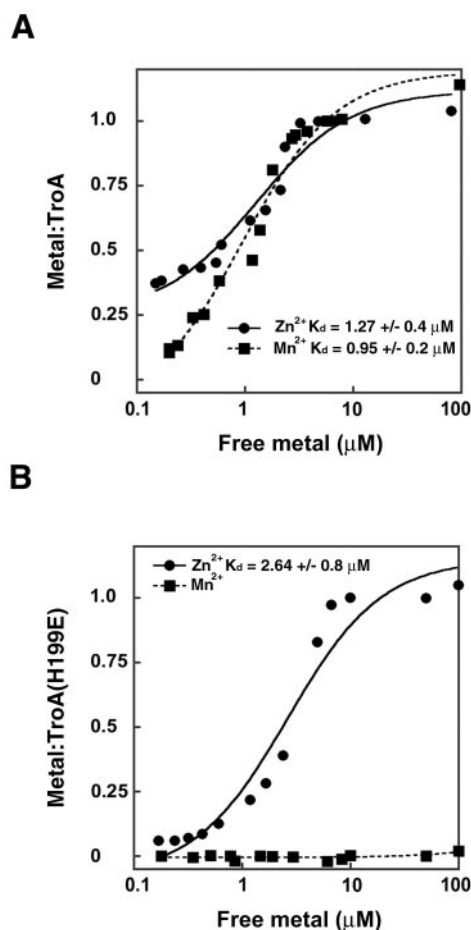


FIG. 2. Binding of Zn^{2+} and Mn^{2+} by wild type (A) and H199E (B) TroA.

four permease genes were expressed in *E. coli* in an arabinose-dependent manner (data not shown). Next, we sought to determine whether pTroA-D could complement growth defects conferred by metal transporter mutations. We initially chose to work with *Y. pestis*, which has been extensively utilized in previous metal transporter studies (34). In addition to a strain harboring a mutation in the Fe^{3+}/Mn^{2+} transporter, Yfe, (34), we used allelic replacement to generate mutations in the Znu (Zn^{2+}) (43) and MntH (Mn^{2+}) (40, 44) transporters. The *znu* mutant and *yfe/mntH* double mutant displayed growth defects in metal-restricted broth medium that were corrected by the addition of Zn^{2+} and Mn^{2+} , respectively; as reported previously for *S. typhimurium* and *E. coli* (44), mutation of *mntH* alone caused no discernible growth defect (data not shown). Expression of the Tro transporter, confirmed by immunoblot analysis for TroA (data not shown), failed to improve the growth of either the *znu* or *yfe/mntH* mutants, whereas expression of the homologous Znu or MntH permeases from plasmids pZnu2 and pMntH-Op (see the supplemental table) restored wild type growth (Fig. 3A). We also used an assay format in which bacterial strains are streaked onto solid medium containing increasing concentrations of iron or Zn^{2+} chelators (34). Growth of the *yfe* and *znu* mutants into the metal-depleted zone was enhanced by the plasmid-borne *Y. pestis* Yfe (pYfe3) (34) and Znu permeases but not by the Tro transporter (Fig. 3B). The lack of a manganese-specific chelator precluded a similar examination of Mn^{2+} uptake.

Finally, we utilized a Zn^{2+} uptake-deficient strain of *E. coli* (38) to assess Zn^{2+} -dependent complementation by the Tro permease. As with the *znu* mutant *Y. pestis*, growth of the

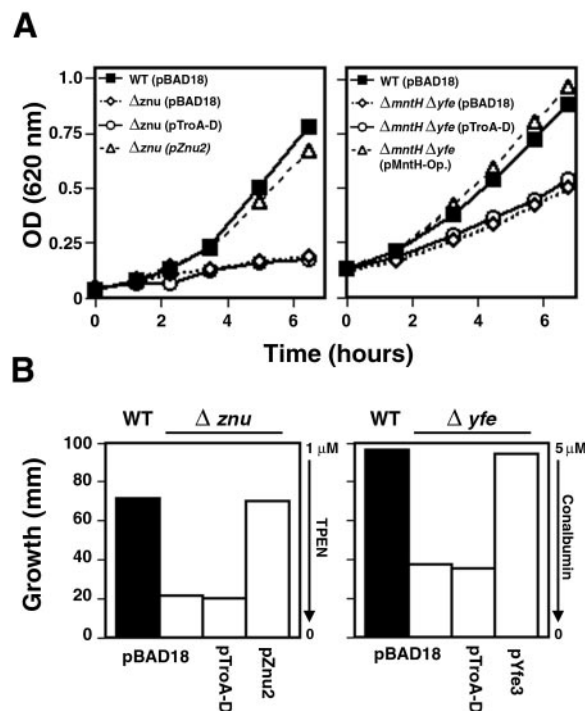


FIG. 3. Phenotypic analysis of Tro permease expression in *Y. pestis* metal transporter mutants. A, expression of the Tro permease in *Y. pestis* Zn^{2+} and Mn^{2+} transporter mutant strains fails to restore wild type growth in metal-restricted broth. B, expression of the homologous Znu and Yfe transporters, but not the Tro permease, restores wild type growth against gradients of Zn^{2+} (TPEN) and iron (conalbumin) chelators, respectively.

$\Delta znu/\Delta zupT$ double mutant strain of *E. coli* in Zn^{2+} -restricted broth medium was corrected by either the addition of Zn^{2+} or expression of the native Znu transporter (pEc Znu; supplemental table) but not by expression of the Tro genes (pTroA-D) (data not shown). Because *E. coli* Mn^{2+} uptake mutants have no discernible growth defect (39, 40), a similar analysis of Mn^{2+} -dependent complementation was not performed.

To assess Tro-mediated metal transport more directly, we sought to detect uptake of isotopically labeled Zn^{2+} and Mn^{2+} in *E. coli*. Because potentially poor heterologous function could hinder detection of uptake, these assays were performed in strains deficient in metal transporters that were grown in medium depleted of metal to reduce internal stores. In a strain lacking all known Zn^{2+} uptake and efflux systems (38), the Tro permease reproducibly promoted modest uptake of $^{65}Zn^{2+}$ (~3-fold above background), confirming the functionality of the transporter; in parallel assays using a *mntH* mutant strain (40), we detected a similar degree of $^{54}Mn^{2+}$ uptake by the Tro transporter (data not shown). Because complementation of a *znu* mutant *E. coli* by the homologous zinc transporter has been reported to be accompanied by an approximate 20-fold increase in $^{65}Zn^{2+}$ uptake (43), it seems likely that the 3-fold increase of $^{65}Zn^{2+}$ uptake by the heterologously expressed Tro permease was not sufficient for complementation. Poor permease expression seemed a likely explanation for the low levels of metal uptake; indeed, immunoblot analysis revealed that TroA levels were ~10- and 20-fold lower on a per cell basis in arabinose-induced *E. coli* (pTroA-D) and *Y. pestis* (pTroA-D), respectively, than in *T. pallidum* (data not shown).

Given the above evidence of poor heterologous function by the Tro transporter, we hypothesized that metal transport activity might be more readily discernible by assaying for enhanced growth inhibition during incubation with high concentrations of exogenous metals (22, 38, 40, 44–46). For these

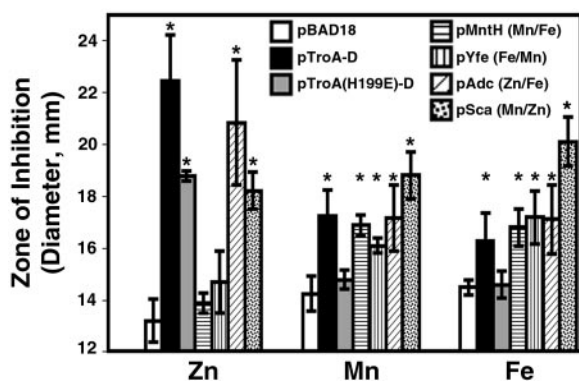


FIG. 4. Expression of the Tro transporter renders *E. coli* hypersensitive to Zn^{2+} , Mn^{2+} , and iron. Wild type *E. coli* harboring the indicated plasmids were plated on HRMM/arabinose agar and exposed to sterile disks impregnated with $ZnCl_2$, $MnCl_2$, or $FeSO_4$. The asterisks indicate values (means and standard deviations) that are significantly different ($p < 0.01$, $n = 3-7$) from those of the vector control for each metal. Primary and secondary metal substrates of previously characterized transporters are indicated in parentheses.

experiments, we chose to employ disk diffusion assays in which enhanced metal uptake is manifested within a lawn of bacteria as an increased zone of inhibition surrounding a metal-containing disk (44, 46). As controls, several previously characterized metal transporters, namely, Adc of *S. pneumoniae* (Zn^{2+}) (47), MntH of *E. coli* (Mn^{2+}) (40, 44), Sca of *S. gordonii* (Mn^{2+}) (48), and Yfe (Fe^{3+}/Mn^{2+}) were cloned into pBAD18. The combined results for these experiments are presented in Fig. 4. Expression of the Tro and Adc permeases significantly enhanced Zn^{2+} -dependent growth inhibition as compared with the pBAD18 vector or constructs expressing MntH or Yfe, neither of which appear to mediate $^{65}Zn^{2+}$ uptake. Expression of a Tro transporter harboring the H199E TroA mutation also resulted in increased Zn^{2+} -dependent growth inhibition, suggesting that the mutant SBP retained a near wild type conformation. Expression of Sca also enhanced Zn^{2+} -dependent growth inhibition, consistent with Zn^{2+} inhibition of Sca-mediated Mn^{2+} uptake (48). Consistent with our binding data, Mn^{2+} -dependent growth inhibition of transformants expressing the wild type, but not the H199E mutant, Tro transporter was comparable with that displayed by cells expressing MntH, Yfe, Sca, and Adc. Similarly, expression of the wild type, but not the mutant Tro permease, resulted in enhanced growth inhibition by iron, as did expression of MntH, Yfe, Sca, and Adc. These findings are in accord with the ability of the MntH and Yfe permeases to transport iron (34, 40, 44) and the ability of Fe^{3+} to partially rescue Adc mutants (47).

Zn^{2+} Represses the tro Operon in Vivo at Much Lower Concentrations than Does Mn^{2+} —Gherardini and co-workers (20) reported that TroR is activated exclusively by Mn^{2+} *in vitro*. They also showed that expression of TroR could repress a *tro* promoter-*lacZ* reporter in *E. coli*, although they were unable to demonstrate metal dependence of TroR function *in vivo*. The Zn^{2+} binding and transport data reported above prompted us to re-examine the role of Zn^{2+} in TroR activation. We again used *E. coli* as a surrogate host for regulation studies. However, rather than expressing *troR* from an inducible strong promoter (20), we cloned the entire *tro* operon with its promoter into the very low copy number plasmid pWSK129 (36) generating pPro-Gpm. We reasoned that this construct would better mimic native TroR-*tro* promoter interactions and, at the same time, allow examination of *gpm* expression when the *tro* promoter is repressed.

Immunoblot and RT-PCR analyses confirmed that all of the *tro* genes were expressed by *E. coli* pPro-Gpm transformants

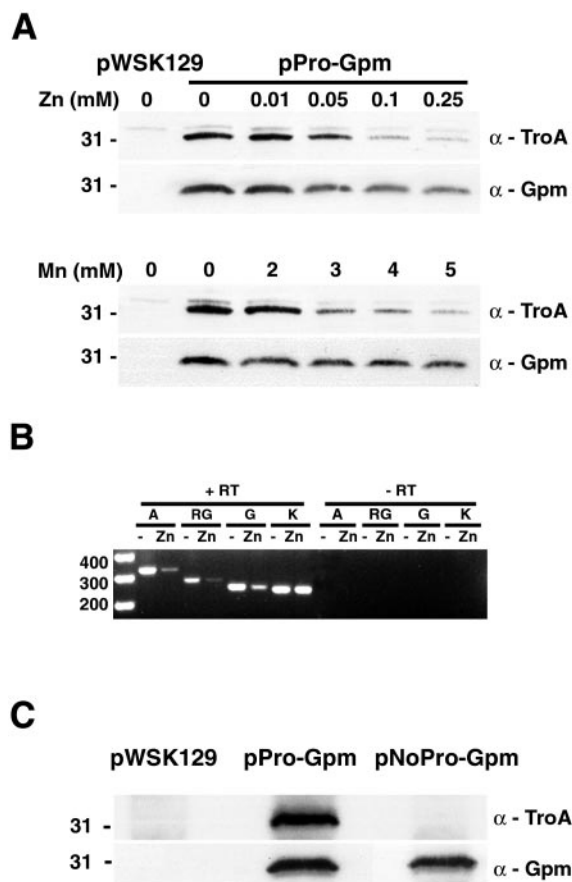


FIG. 5. Heterologous metal-dependent repression of the tro genes *in vivo*. A, *E. coli* (pPro-Gpm) was grown to late-log phase in HRMM containing the indicated concentrations of exogenous $ZnCl_2$ or $MnCl_2$ and analyzed for TroA and Gpm expression by immunoblot. B, detection of *tro* transcripts in *E. coli* (pPro-Gpm) grown in the absence (-) or presence (+) of 0.5 mM $ZnCl_2$. 1 ng of RNA/reaction was analyzed by RT-PCR (+RT) using primers specific for *troA* (lanes A), the *troR-gpm* intergenic region (lanes RG), *gpm* (lanes G), and the vector-encoded kanamycin-resistance gene (lanes K). PCR amplification with 1 ng of RNA/reaction (-RT) served as a negative control. C, Gpm is expressed in the absence of the *tro* promoter. *E. coli* transformants harboring pWSK129, pPro-Gpm, or pNoPro-Gpm were grown to late-log phase in HRMM and analyzed for TroA and Gpm expression by immunoblot. Protein (kDa) and DNA (bp) markers are indicated on the left. The membranes in A and C were developed for TroA, stripped, and re-probed for Gpm.

(data not shown). Interestingly, unlike TroA and Gpm, which are readily detectable by immunoblot analysis, TroR could not be detected in either *E. coli*(pPro-Gpm) or *T. pallidum* by enhanced chemiluminescence (data not shown). Because transcriptional repressor proteins are typically found in very low abundance (23), these results supported the use of *E. coli* as a *T. pallidum* surrogate. As shown in Fig. 5A, Zn^{2+} -mediated repression of TroA was apparent at 50 μM , whereas much higher concentrations of Mn^{2+} (> 2 mM) were required to effect a comparable repression. Iron concentrations up to 500 μM had no discernable effect on TroA expression (data not shown). By plotting the exogenous metal concentrations against the intensity of the TroA bands, we calculated mean EC_{50} values for Zn^{2+} and Mn^{2+} repression of TroA of 71 μM and 2.66 mM, respectively (data not shown). To increase the sensitivity of these assays, particularly for Mn^{2+} , we next performed repression studies using strains of *E. coli* that had been engineered to have elevated levels of intracellular Zn^{2+} and Mn^{2+} . In an *E. coli* strain defective for Zn^{2+} efflux ($\Delta zntA/\Delta zitB$) (38), Zn^{2+} -mediated repression of TroA was apparent at 10 μM and abso-

TABLE I
Orthologs in the *T. pallidum* genome

Protein	<i>T. pallidum</i> gene number
Orthologs of transition metal-dependent enzymes	
Zinc	
DNA topoisomerase I	TP0394
DNA primase	TP0492
RNA polymerase β'	TP0242
Adenosine deaminase	TP0045
5' nucleotidase	TP0104
Threonyl-tRNA synthetase	TP0837
Methionyl-tRNA synthetase	TP0798
Isoleucyl-tRNA synthetase	TP0452
	TP0112
Aminopeptidases	
	TP0842
	TP0842
Zinc protease	TP0600
α -Amylase	TP0147
	TP0221
Carboxypeptidases	
	TP0574 ^a
	TP0800
Fructose-biphosphate aldolase	TP0662
Enolase	TP0817
Iron	
Ribonucleoside-diphosphate reductase β'	TP0053
Bacteroferrin	TP1038
Neelaredoxin (superoxide reductase)	TP0823 ^a
Rubredoxin	TP0991 ^a
Pyruvate oxidoreductase	TP0939
Quinoline 2-oxidoreductase	TP0080
Methionine aminopeptidase	TP0842
Manganese	
Phosphoenolpyruvate carboxykinase	TP0122
	TP0218
PP2C-like phosphatases	TP0219
Aminopeptidase P	TP0569
Orthologs of metal transporters	
TroABCD	TP0163–TP0166
C9 ABC Permease	TP0034–TP0036
Mg ²⁺ uptake (MgtE)	TP0917
Na ⁺ /K ⁺ uptake pumps (NtpJ and TrkA)	TP0140, TP0513
Na ⁺ efflux-oxaloacetate decarboxylase subunits	TP0056, TP0057
Metal (Cu ²⁺ ?) efflux pump, P-type ATPase	TP1036

^a *T. pallidum* proteins which have been shown to bind the indicated metal.

lute at 50 μM Zn²⁺ (supplemental Fig. S2). In contrast, Mn²⁺-dependent repression in a MntH-overexpressing strain of *E. coli* was apparent at 50 μM Mn²⁺ and only 70% complete at 250 μM Mn²⁺ (supplemental Fig. S2), further suggesting that TroR is primarily Zn²⁺-responsive. Interestingly, repression of TroA was not accompanied by a commensurate decrease in Gpm (Fig. 5A). Densitometric analysis revealed that Gpm decreased by ~50% under conditions that resulted in a greater than 90% decrease of TroA (data not shown). Separate immunoblot experiments using antibodies directed against the constitutively expressed σ^{70} protein were used as loading controls (data not shown). To confirm that these protein data were indicative of changes in *tro* transcript levels, RT-PCR analysis was performed using primers specific for *troA*, the *troR-gpm* intergenic region, and the *gpm* coding region. Consistent with the above results, growth of *E. coli* (pPro-Gpm) in the presence of exogenous Zn²⁺ resulted in marked reductions of *troA* and *troR-gpm* transcripts (84 and 88% decrements, respectively; Fig. 5B). In contrast, *gpm* mRNA levels were reduced by 55%, whereas those of the vector-encoded kanamycin resistance gene were effectively unchanged (1.5% reduction). These results point to the existence of an autonomous *gpm* promoter. To confirm this, we performed immunoblot analysis on *E. coli* bearing a variant of plasmid pPro-Gpm, dubbed pNoPro-Gpm, which lacks the *tro* promoter. *E. coli* (pNoPro-Gpm) contained readily detectable levels of Gpm, whereas TroA, as expected, was not detected (Fig. 5C). By performing a similar analysis with constructs lacking various amounts of sequence upstream of *gpm*, the

autonomous *gpm* promoter activity was localized to 541 bp of DNA directly upstream of the *gpm* start codon (data not shown).

DISCUSSION

In this report, we used metal binding analysis of apo-TroA in conjunction with *in vivo* heterologous systems to define the function and regulation of the Tro transporter. Collectively, our findings indicate that the Tro permease transports Zn²⁺, Mn²⁺, and possibly iron but is primarily regulated by Zn²⁺. Moreover, expression of *gpm* is partially independent of metal-dependent repression. Given the concentrations of these metals within human body fluids, we conclude that Zn²⁺, not Mn²⁺, is both the primary substrate and co-repressor of the Tro transporter.

As a platform for understanding the contribution of the Tro permease to transition metal homeostasis in *T. pallidum*, we surveyed the genome of the spirochete (9) for orthologs of known metal-dependent enzymes and metal transporters (Table I). As noted, *T. pallidum* lacks many iron-dependent proteins found in other bacteria; accordingly, the spirochete also lacks siderophore biosynthetic genes and dedicated iron uptake systems. Because Zn²⁺ is second in abundance only to iron within other bacteria, as well as within the obligate human host of the spirochete (41), the small number of iron metalloproteins in *T. pallidum* suggests that Zn²⁺ is likely the predominant transition metal in the bacterium. Indeed, a number of abundantly expressed putative Zn²⁺ metalloproteins partic-

ipate in a variety of crucial cellular processes involving nucleic acid and protein synthesis/degradation, remodeling of peptidoglycan, and glycolysis (49, 50). Although the intuition that *T. pallidum* requires significant amounts of Mn^{2+} (20) has become widely accepted in the literature (5–7, 21–24), our survey of the genome lends little support to this notion. We were able to identify only four orthologs of known Mn^{2+} -dependent enzymes, whereas a number of well characterized Mn^{2+} -metalloproteins, such as PrpA and PrpB protein phosphatases, Pkn2/PknA type kinases, family II inorganic pyrophosphatase, sphingomyelinase, phosphatidylserine synthase, Mn^{2+} -fructose-1,6-bisphosphate phosphatase (GlpX), L-fucose isomerase, cellobiose-6-phosphate hydrolase, arginase/agmatinase, pyruvate carboxylase, glutamine synthetase, Mn^{2+} -RNaseH, SpoT, superoxide dismutase, catalase, and Mn^{2+} -peroxidase (7) are notably absent. Unlike the phylogenetically distinct Mn^{2+} -dependent enzymes of several *Bacillus* species, the treponemal Gpm has recently been demonstrated to have no requirement for Mn^{2+} (16). Significantly, *T. pallidum* does not encode orthologs of either of the Mn^{2+} transporters MntH or the P-type ATPase, MntA.

The equal affinity of TroA for both Zn^{2+} and Mn^{2+} ($K_d \approx 1 \mu M$) suggests that the Tro permease could transport multiple metals. Notably, these affinities are similar to those of several other C9 permeases measured in whole cell radioisotope uptake studies (39, 48, 51). To extend these *in vitro* binding studies, we heterologously expressed the Tro transporter in the surrogate hosts *Y. pestis* and *E. coli*. Despite the inability of the Tro permease to complement the growth defects of *Y. pestis* and *E. coli* transporter mutants, likely because of poor heterologous expression and/or function, we were clearly able to discern transport activity in *E. coli* by assaying for $^{65}Zn^{2+}$ and $^{54}Mn^{2+}$ uptake and increased growth inhibition by Zn^{2+} , Mn^{2+} , and iron. Thus, the *in vitro* binding experiments and the *in vivo* functional analyses yield internally consistent data indicating that the Tro permease plays an important role in fulfilling the requirements of the spirochete for Zn^{2+} , Mn^{2+} , and possibly iron. Interestingly, among the C9 permeases, the capacity for transporting multiple metals appears to be a more common feature than is generally appreciated. In the only other analysis of multiple metal binding by a purified C9 SBP, the streptococcal MtsA protein was found to bind Zn^{2+} , Fe^{3+} , and Cu^{2+} , whereas the intact permease transported both Fe^{3+} and Zn^{2+} (52). The *Y. pestis* Yfe and *S. parasanguis* Fim permeases transported both Fe^{3+} and Mn^{2+} (34, 53). Mutation of the *S. pneumoniae* Adc permease imparts a growth defect that is corrected primarily by Zn^{2+} , and to lesser degrees by Cu^{2+} and Fe^{2+} (47). Finally, Zn^{2+} is a potent competitive inhibitor of Mn^{2+} uptake by the Sca, Sit, and Mnt ATP-binding cassette permeases (39, 48, 51). Because Zn^{2+} and iron can be bound with coordination numbers of either 4, 5, or 6, whereas Mn^{2+} can be coordinated through five or six binding interactions (54, 55), it is not surprising that many of the C9 SBPs, all of which have residues consistent with either a pentavalent or hexacoordinate ligand binding site, would be able to bind multiple metals.

Examination of the local architectures of the ligand-binding sites of TroA and PsaA revealed by the crystal structures (15, 42) enables us to explain the counter-intuitive observation that TroA (H199E) failed to bind manganese. Among the C9 SBPs containing His¹⁹⁹, this amino acid is flanked on one or both sides by a bulky (Phe or Gln) or a negatively charged (Asp) residue (supplemental Fig. S1). In contrast, the flanking residues of the Glu¹⁹⁹ subgroup of C9 SBPs are small (Gly, Ser, or Cys), thereby affording the carboxylate moiety the mobility to form bidentate interactions with the bound metal. The residues

flanking His¹⁹⁹ likely constrain and orient the N δ -H tautomer of His¹⁹⁹, thereby promoting a favorable interaction of the N ϵ 2 atom with the coordinated metal (54). We hypothesize that by placing a Glu in this constraining environment, only a single carboxylate oxygen can interact with the bound metal. Moreover, the spatial proximity of residue 199 to His¹³³ (15) would allow the remaining carboxylate oxygen of Glu¹⁹⁹ to interact with the N ϵ 2 atom of His¹³³, thereby preventing His¹³³ from binding the coordinated metal. If so, the H199E mutation would actually impart a tetrahedral coordination geometry that is not conducive for Mn^{2+} binding but is frequently utilized in Zn^{2+} -binding proteins (54, 55). The observation that TroA(H199E) binds Zn^{2+} but not Mn^{2+} suggests that the wild type TroA sequence has been maintained through a selective pressure favoring multiple metal binding capacity.

By cloning the entire *tro* operon into a very low copy number plasmid, we were able to observe TroR-mediated repression of the *tro* genes *in vivo* in response to physiologically relevant concentrations of Zn^{2+} , whereas supraphysiological (>2 mM) concentrations of Mn^{2+} were required to effect a similar down-regulation. The concentrations of Zn^{2+} required to activate TroR ($\sim 70 \mu M$) are close to those ($\sim 10 \mu M$) that activate the *E. coli* Zn^{2+} -dependent transcriptional repressor, Zur (23). Whether the slightly higher levels of Zn^{2+} required to activate TroR represents a true “evolutionary tuning” of TroR to a higher intracellular Zn^{2+} content or merely an effect of the copy number (approximately seven) (36) of the plasmid pPro-Gpm remains to be seen. In stark contrast, the levels of Mn^{2+} required to activate TroR (~ 2 mM) are 2000-fold greater than those ($\sim 10 \mu M$) that activate the *E. coli* Mn^{2+} -dependent repressor MntR (56). Thus, we conclude that Zn^{2+} is the native co-repressor of the *tro* genes, in contrast to Posey *et al.* (20), who reported that TroR purified from inclusion bodies and renatured was exclusively activated by Mn^{2+} *in vitro*. The observation that both the *E. coli* and *Bacillus subtilis* Zur proteins, when purified from inclusion bodies and renatured, are activated by Zn^{2+} and Mn^{2+} *in vitro*, whereas neither of these Zn^{2+} -dependent repressors responds to Mn^{2+} *in vivo* (27, 28) lends a cautionary note to results obtained with denatured/renatured repressor proteins used for *in vitro* assays. Based on the premise that TroR is activated by Mn^{2+} (20), it was suggested that repression of the *tro* operon was likely to occur during infection of the central nervous system. However, as a sexually transmitted pathogen, *T. pallidum* is frequently exposed to semen, which contains very high levels of Zn^{2+} (~ 1 to 2 mM) (57–59). Based on our findings, we suggest that Zn^{2+} -mediated repression during exposure to semen is a more plausible scenario. As spirochetes disseminate from the site of inoculation and encounter much lower levels of Zn^{2+} , such as those present in serum and cerebrospinal fluid (~ 15 and $\sim 2 \mu M$, respectively) (60, 61), repression of the Tro permease would be alleviated.

The detection of *troR-gpm* co-transcripts by RT-PCR prompted the notion that Gpm expression was exclusively dependent upon transcription from the *tro* promoter (13). Gherardini and co-workers (16, 20) further suggested that TroR-mediated repression of Gpm within the central nervous system would decrease treponemal metabolism and thereby contribute to the latency of syphilitic infection. Because *T. pallidum* can only generate ATP by glycolysis, such a genetic arrangement seems inherently problematic because TroR-mediated repression of Gpm would hinder generation of ATP and thus the ability of the bacterium to escape a potentially metal-toxic environment. Consistent with the notion that glycolysis must proceed during TroR-mediated repression, we observed that Gpm expression continues when activity from the *tro* promoter

is abolished. We postulate, therefore, that the net expression of *gpm* cumulatively results from transcriptional read-through from the *tro* promoter as well as from an autonomous *gpm*-specific promoter. Precedent for this type of genetic arrangement is provided by the streptococcal C9 permeases Sca, Fim, Adc, and Psa, all of which contain a downstream gene unassociated with either the transporter or its repressor that is expressed from both the permease promoter and from an autonomous promoter (45, 47, 62, 63). This observation, however, does not explain the physiological relevance of this genetic arrangement. We can only speculate that the level of Gpm activity that occurs during repression of the Tro permease is sufficient to meet the metabolic needs of the spirochete. Regardless of its transcriptional control, the prevalence of an unrelated protein in multiple C9 permease operons suggests that its presence is not coincidental, implying some currently unknown physiological advantage.

Acknowledgments—We thank Melissa J. Caimano and Christian H. Eggers for critical review of this manuscript, Christian H. Eggers and Constance Pope for technical assistance, Glenn F. King for help with calculating dissociation constants, and Christopher Rensing (University of Arizona) for providing *E. coli* strains.

REFERENCES

- Tramont, E. C. (2000) in *Principles and Practice of Infectious Diseases* (Mandell, G. L., Bennett, J. E., and Dolin, R., eds) pp. 2474–2490, Churchill Livingstone, Inc., New York
- Payne, S. M. (1993) *Trends Microbiol.* **1**, 66–69
- Ratledge, C., and Dover, L. G. (2000) *Annu. Rev. Microbiol.* **54**, 881–941
- Vasil, M. L., and Ochsner, U. A. (1999) *Mol. Microbiol.* **34**, 399–413
- Claverys, J.-P. (2001) *Res. Microbiol.* **152**, 231–243
- Hantke, K. (2001) *Biometals* **14**, 239–249
- Jakubovics, N. S., and Jenkinson, H. F. (2001) *Microbiology* **147**, 1709–1718
- Bhattacharyya-Pakrasi, M., Pakrasi, H. B., Ogawa, T., and Aurora, R. (2002) *Biochem. Soc. Trans.* **30**, 768–770
- Fraser, C. M., Norris, S. J., Weinstock, G. M., White, O., Sutton, G. G., Dodson, R., Gwinn, M., Hickey, E. K., Clayton, R., Ketchum, K. A., Sodergren, E., Hardham, J. M., McLeod, M. P., Salzberg, S., Peterson, J., Khalak, H., Richardson, D., Howell, J. K., Chidambaram, M., Utterback, T., McDonald, L., Artiach, P., Bowman, C., Cotton, M. D., and Venter, J. C. (1998) *Science* **281**, 375–388
- Jovanovic, T., Ascenso, C., Hazlett, K. R. O., Sikkink, R., Krebs, C., Litwiller, R., Benson, L. M., Moura, I., Moura, J. J. G., Radolf, J. D., Huynh, B. H., and Rusnak, F. (2000) *J. Biol. Chem.* **275**, 28439–28448
- Lombard, M., Touati, D., Fontecave, M., and Niviere, V. (2000) *J. Biol. Chem.* **275**, 27021–27026
- Hazlett, K. R. O., Cox, D. L., Sikkink, R. A., Auch'ere, F., Rusnak, F., and Radolf, J. D. (2002) *Methods Enzymol.* **353**, 140–156
- Hardham, J. M., Stamm, L. V., Porcella, S. F., Frye, J. G., Barnes, N. Y., Howell, J. K., Mueller, S. L., Radolf, J. D., Weinstock, G. M., and Norris, S. J. (1997) *Gene (Amst.)* **197**, 47–64
- Akins, D. R., Robinson, E., Shevchenko, D., Elkins, C., Cox, D. L., and Radolf, J. D. (1997) *J. Bacteriol.* **179**, 5076–5086
- Lee, Y. H., Deka, R. K., Norgard, M. V., Radolf, J. D., and Hasemann, C. A. (1999) *Nat. Struct. Biol.* **6**, 628–633
- Benoit, S., Posey, J. E., Chenoweth, M. R., and Gherardini, F. C. (2001) *J. Bacteriol.* **183**, 4702–4708
- Deka, R. K., Lee, Y. H., Hagman, K. E., Shevchenko, D., Lingwood, C. A., Hasemann, C. A., Norgard, M. V., and Radolf, J. D. (1999) *J. Bacteriol.* **181**, 4420–4423
- Tam, R., and Saier, M. H., Jr. (1993) *Microbiol. Rev.* **57**, 320–346
- Higgins, C. F. (2001) *Res. Microbiol.* **152**, 205–210
- Posey, J. E., Hardham, J. M., Norris, S. J., and Gherardini, F. C. (1999) *Proc. Natl. Acad. Sci. U. S. A.* **96**, 10887–10892
- Horsburgh, M. J., Clements, M. O., Crossley, H., Ingham, E., and Foster, S. J. (2001) *Infect. Immun.* **69**, 3744–3754
- Horsburgh, M. J., Wharton, S. J., Cox, A. G., Ingham, E., Peacock, S., and Foster, S. J. (2002) *Mol. Microbiol.* **44**, 1269–1286
- Hantke, K. (2001) *Curr. Opin. Microbiol.* **4**, 172–177
- Kitten, T., Munro, C. L., Michalek, S. M., and Macrina, F. L. (2000) *Infect. Immun.* **68**, 4441–4451
- Eidsness, M. K., O'Dell, S. E., Kurtz, D. M., Jr., Robson, R. L., and Scott, R. A. (1992) *Protein. Eng.* **5**, 367–371
- Petitot, Y., Forest, E., Mathieu, I., Meyer, J., and Moulis, J. M. (1993) *Biochem. J.* **296**, 657–661
- Gaballa, A., and Helmann, J. D. (1998) *J. Bacteriol.* **180**, 5815–5821
- Patzer, S. I., and Hantke, K. (2000) *J. Biol. Chem.* **275**, 24321–24332
- Hazlett, K. R. O., Sellati, T. J., Nguyen, T. T., Cox, D. L., Clawson, M. L., Caimano, M. J., and Radolf, J. D. (2001) *J. Exp. Med.* **193**, 1015–1026
- Gong, S., Bearden, S. W., Geoffroy, V. A., Fetherston, J. D., and Perry, R. D. (2001) *Infect. Immun.* **69**, 2829–2837
- Lee, Y. H., Dorwart, M. R., Hazlett, K. R. O., Deka, R. K., Norgard, M. V., Radolf, J. D., and Hasemann, C. A. (2002) *J. Bacteriol.* **184**, 2300–2304
- Pendrak, M. L., and Perry, R. D. (1991) *Biol. Amst.* **4**, 41–47
- Fetherston, J. D., Bertolino, V. J., and Perry, R. D. (1999) *Mol. Microbiol.* **32**, 289–299
- Bearden, S. W., and Perry, R. D. (1999) *Mol. Microbiol.* **32**, 403–414
- Sarker, M. R., and Cornelis, G. R. (1997) *Mol. Microbiol.* **23**, 410–411
- Wang, R. F., and Kushner, S. R. (1991) *Gene (Amst.)* **100**, 195–199
- Guzman, L. M., Belin, D., Carson, M. J., and Beckwith, J. (1995) *J. Bacteriol.* **177**, 4121–4130
- Grass, G., Wong, M. D., Rosen, B. P., Smith, R. L., and Rensing, C. (2002) *J. Bacteriol.* **184**, 864–866
- Kehres, D. G., Janakiraman, A., Slauch, J. M., and Maguire, M. E. (2002) *J. Bacteriol.* **184**, 3159–3166
- Kehres, D. G., Zaharik, M. L., Finlay, B. B., and Maguire, M. E. (2000) *Mol. Microbiol.* **36**, 1085–1100
- Outten, C. E., and O'Halloran, T. V. (2001) *Science* **292**, 2488–2492
- Lawrence, M. C., Pilling, P. A., Epa, V. C., Berry, A. M., Ogunniyi, A. D., and Paton, J. C. (1998) *Structure* **6**, 1553–1561
- Patzer, S. I., and Hantke, K. (1998) *Mol. Microbiol.* **28**, 1199–1210
- Makui, H., Roig, E., Cole, S. T., Helmann, J. D., Gros, P., and Cellier, M. F. (2000) *Mol. Microbiol.* **35**, 1065–1078
- Jakubovics, N. S., Smith, A. W., and Jenkinson, H. F. (2000) *Mol. Microbiol.* **38**, 140–153
- Que, Q., and Helmann, J. D. (2000) *Mol. Microbiol.* **35**, 1454–1468
- Dintilhac, A., Alloing, G., Granadel, C., and Claverys, J.-P. (1997) *Mol. Microbiol.* **25**, 727–739
- Kolenbrander, P. E., Andersen, R. N., Baker, R. A., and Jenkinson, H. F. (1997) *J. Bacteriol.* **180**, 290–295
- Deka, R. K., Machius, M., Norgard, M. V., and Tomchick, D. R. (2002) *J. Biol. Chem.* **277**, 41857–41864
- Bremer, H., and Dennis, P. P. (1996) in *Escherichia coli and Salmonella typhimurium Cellular and Molecular Biology* (Neidhardt, F. C., Ingraham, J. L., Low, K. B., Magasanik, B., Schaechter, M., and Umberger, H. E., eds) pp. 1553–1569, American Society for Microbiology, Washington, D.C.
- Bartsevich, V. V., and Pakrasi, H. B. (1996) *J. Biol. Chem.* **271**, 26057–26061
- Janulczyk, R., Fallon, J., and Björck, L. (1999) *Mol. Microbiol.* **34**, 596–606
- Oetjen, J., Fives-Taylor, P., and Froeliger, E. H. (2002) *Infect. Immun.* **70**, 5706–5714
- Christianson, D. W. (1997) *Prog. Biophys. Mol. Biol.* **67**, 217–252
- Alberts, I. L., Nadassy, K., and Wodak, S. J. (1998) *Protein Sci.* **7**, 1700–1716
- Patzer, S. I., and Hantke, K. (2001) *J. Bacteriol.* **183**, 4806–4813
- Abou-Shakra, F. R., Ward, N. I., and Everard, D. M. (1989) *Fertil. Steril.* **52**, 307–310
- Umeyama, T., Ishikawa, H., Takeshima, H., Yoshii, S., and Koiso, K. (1986) *Fertil. Steril.* **46**, 494–499
- Vallee, B. L. (1959) *Physiol. Rev.* **39**, 443–490
- Jimenez-Jimenez, F. J., Molina, J. A., Aguilar, M. V., Meseguer, I., Mateos-Vega, C. J., Gonzalez-Munoz, M. J., de Bustos, F., Martinez-Salio, A., Orti-Pareja, M., Zurdo, M., and Martinez-Para, M. C. (1998) *J. Neural Transm.* **105**, 497–505
- Molina, J. A., Jimenez-Jimenez, F. J., Aguilar, M. V., Meseguer, I., Mateos-Vega, C. J., Gonzalez-Munoz, M. J., de Bustos, F., Porta, J., Orti-Pareja, M., Zurdo, M., Barrios, E., and Martinez-Para, M. C. (1998) *J. Neural Transm.* **105**, 479–488
- Fenno, J. C., Shaikh, A., Spatafora, G., and Fives-Taylor, P. (1995) *Mol. Microbiol.* **15**, 849–863
- Novak, R., Braun, J. S., Charpentier, E., and Tuomanen, E. (1998) *Mol. Microbiol.* **29**, 1285–1296